Adsorption (2009) 15: 300–305
DOI 10.1007/s10450-009-9183-8

Study of structure properties of organized silica sorbents synthesized on polymeric templates

Adam W. Marczewski · Anna Derylo-Marczewska · Iwona Skrzypek · Stanislaw Pikus · Maciej Kozak

Published online: 31 March 2009

Abstract Mesoporous silica materials were synthesized by applying Pluronic type polymers as pore creating agents. The composition of a reacting mixture and the process conditions were changed in a synthesis procedure. These changes differentiated the characteristics of porous structure of obtained sorbents. The parameters characterizing the pore structure were estimated and the changes of pore arrangement of obtained materials being a result of different synthesis conditions were investigated. The small-angle XRD results indicate that *F* cubic structure was formed what confirms the cage-like ordering of the synthesized silicas.

Keywords Mesoporous silicas · Kinetics of adsorption from solution

1 Introduction

New technique of synthesis of molecular sieves of larger diameters between micropores and macropores is based on usage of self-organized surfactant solutions as template agents (Zhao et al. 1998; Krämer et al. 1998; Schmidt-Winkel et al. 1999a, 1999b; Schmidt-Winkel et al. 2000; Coleman et al. 2001; Melosh et al. 2001; Hartmann and Vinu 2002; Newalkar and Komarneni 2002; Janssen et al. 2002). The structure of the materials depends on a type of used template (various surfactants, polymers, liquid crystals), the synthesis conditions (composition of a reacting mixture, addition of a pore expanding agent) or a post-synthesis treatment (temperature and duration of aging process). The SBA-15 or MCF materials belonging to silicas of wider mesopore system are synthesized by applying the polymer templates. They receive much attention because of the possibility of application in the catalytic processes involving large molecules (Han et al. 2001). Among such adsorbents the cage-like ordered silicas seem to be very interesting because of some application reasons, however, the analysis of their porous structure is rather complicated (Yu et al. 2000; Sakamoto et al. 2000; Lettow et al. 2000; Matos et al. 2002; Kruk et al. 2002).

In the paper, the investigations of the effect of synthesis conditions on the changes of porous structure of mesoporous silicas are presented. Several samples of mesoporous silicas of various porous structures were obtained by changing temperature and time of aging process and the ratio of silica and polymer amounts. As the pore creating agent the Pluronic triblock copolymer was applied, and 1,3,5-trimethyl benzene was introduced as pore expanding agent. The synthesized materials were characterized by using low-temperature nitrogen adsorption in order to compare their structure properties. The regularity of pore systems of obtained materials and the changes of their arrangement being a result of different synthesis conditions were investigated by using the small angle X-ray scattering method. Some of the synthesized samples have a system of ink-bottle pores of narrow pore openings and wider internal cages. Kinetic measurements were undertaken to study the effect of widening of pore entrances on the rate of adsorption.

A.W. Marczewski (✉) · A. Derylo-Marczewska · I. Skrzypek · S. Pikus
Faculty of Chemistry, M. Curie-Skłodowska University, 20-031 Lublin, Poland
e-mail: Adam.Marczewski@umcs.lublin.pl

M. Kozak
Department of Macromolecular Physics, A. Mickiewicz University, 61-614 Poznań, Poland

2 Experimental and calculation procedures

2.1 Material preparation

The syntheses followed a procedure being a modification of the method described in the papers (Zhao et al. 1998; Derylo-Marczewska et al. 2008; Derylo-Marczewska et al. 2005). Two non-ionic triblock copolymers Pluronic PE10500—$(EO)_{36}(PO)_{56}(EO)_{36}$ and PE9400—$(EO)_{21}(PO)_{47}(EO)_{21}$ (BASF, Poland) were applied as templates. The synthesis was conducted in strong acidic conditions (1.6 M HCl) and tetraethylorthosilicate (TEOS) was used as silica source. In the standard procedure a weighed amount of copolymer (5 g) was dissolved in 180 ml of HCl solution. Then, weighed amount of 1,3,5-trimethylbenzene (TMB) (5 g) was added and the mixture was stirred vigorously for 45 min at 308 K. In the next stage of procedure 17 g of TEOS was introduced and the mixture was stirred for the next 20 hrs. Three samples were synthesized at different polymer—TEOS mass ratios: 1:3.5, 1:3 and 1:2.5 (the samples were coded respectively as PE10500-1, PE10500-2, and PE10500-3). The aging process was conducted for 24 or 48 hrs (the samples PE9400-24h and PE9400-48h) in autoclave at elevated temperatures (343, 363 and 393 K—the samples PE9400-70, PE9400-90 and PE-9400-120, respectively). The synthesized product was thoroughly washed with bi-distilled water, dried and calcined at 873 K for 6 hrs.

2.2 Material characterization

Nitrogen adsorption/desorption isotherms at 77 K were determined volumetrically using ASAP 2405N analyzer (Micromeritics Corp., Norcross, GA, USA). Before the experiment the adsorbents were degassed (10^{-2} mmHg) at 493 K.

The linear BET plots of adsorption data were used to evaluate the BET specific surface area, S_{BET}. The total pore volume, V_t was assessed from the adsorption at the relative pressure $p/p_o = 0.98$ (Gregg and Sing 1982). To estimate the values of the external (macropore) surface area, S_{ext}, and the primary mesopore volume, V_p, the α_s plot method was used with the macroporous silica gel LiChrospher Si-1000 as a reference non-porous adsorbent (Jaroniec et al. 1999). The calculations of pore size distributions (PSD) followed the Barrett, Joyner and Halenda (BJH) procedure (Gregg and Sing 1982). The adsorption and desorption mesopore diameters were estimated from the PSD maxima.

The diffraction measurements were conducted at room temperature by using the NanoSTAR system (Bruker AXS) with pin-hole collimation and a two-dimensional detector (HiSTAR), mounted on a microfocus X-ray tube with copper anode and equipped with crossed Göbel mirrors. The sample-to-detector distance was 650 mm. The exposure time for a single frame was 5000–10 000 s. The angle 2θ was calibrated by the observation of peaks from silver behenate diffraction pattern (Huang et al. 1993). The intensities were recorded within the range of $0.3° < 2\theta < 4.5°$. The wavelength was equal to 1.54178 Å.

Kinetic experiments were made by applying the UV-Vis spectrophotometer Cary 100 (Varian, Australia) with a flow cell to measure a solute concentration. The aqueous solutions of methylene blue of established initial concentration were contacted with a known amount of silica sample in a specially constructed vessel. The solution was stirred during the experiment by applying a magnetic stirrer. At definite time intervals the solution samples were collected to the flow cell, the UV-Vis spectra were recorded and collected solution was returned to the vessel. The concentration vs. time and the adsorption vs. time profiles were calculated from the obtained spectra. In the kinetic experiments the 0.1–0.315 mm grain fractions were used.

3 Results and discussion

The influence of aging temperature on the structure characteristics of well-organized mesoporous silicas synthesized on Pluronic templates was discussed in our previous paper (Derylo-Marczewska et al. 2005). Strong changes of pore volumes and diameters, as well as transformations of pore arrangement were found. Another important factor influencing the pore system formation in such materials is time of aging process. In Fig. 1 the nitrogen adsorption/desorption isotherms and XRD patterns are compared for two samples synthesized with PE9400 template and aged at 90°C for 24 and 48 hrs. The isotherms for both materials have characteristic shapes with steep adsorption and desorption branches indicating the uniformity of pore sizes, and with very wide hysteresis loops evidencing an ink-bottle type of the pores with narrow entrances and wide cages. The adsorption branches are similar for two obtained samples which suggests a similarity of their cage sizes, however the desorption branch of the isotherm aged for 48 hrs is shifted towards higher relative pressures which means that the increase of aging time leads to widening of pore entrances for this sorbent. It may be explained as a result of stronger dissolution of silica skeleton of the more exposed material in pore necks at these conditions. Moreover, a distinct increase of adsorption values in the range of higher relative pressures is observed for the sorbent aged for 48 hrs which means that the prolonged aging process leads to a high growth of pore volume as a result of dissolution of silica skeleton as well as creation of interconnectivities between the polymer/TMB droplets constructing the main pore systems. These conclusions are confirmed by the analysis of the values of parameters characterizing the porous structure of synthesized mate-

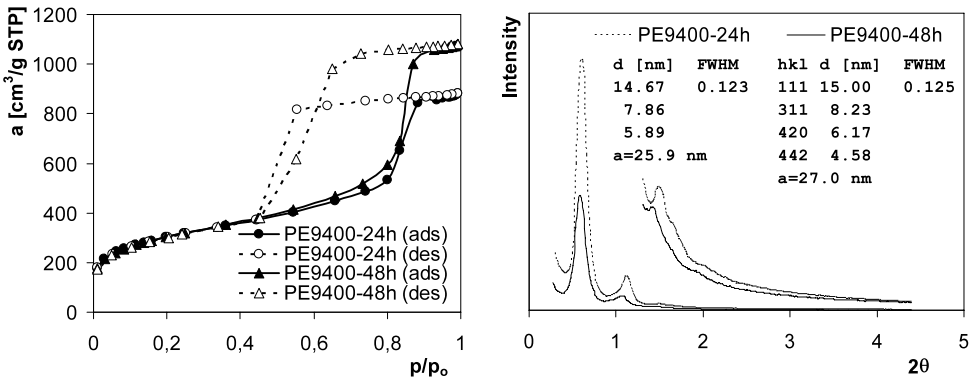

Fig. 1 Nitrogen adsorption/desorption isotherms and small-angle XRD patterns for the mesoporous silicas synthesized on the Pluronic PE9400 template and aged for 24 and 48 hrs

Table 1 Influence of synthesis conditions on the structure characteristics of mesoporous silicas

Sample	S_{BET} [m^2/g]	V_t [cm^3/g]	V_p [cm^3/g]	S_{ext} [m^2/g]	D_a / D_d [nm]	Pores v/v%
PE9400-48h	1079	1.66	1.61	31	13.9 / 4.2	79
PE9400-24h	1082	1.35	1.24	65	11.4/ 3.6	75
PE10500-1	980	0.81	0.78	19	6.8 / 4.1	64
PE10500-2	1081	0.85	0.83	12	6.8 / 4.0	65
PE10500-3	1087	0.90	0.89	6	8.8 / 3.8	66
PE9400-70	814	0.77	0.52	167	7.8 / 4.0	63
PE9400-120	695	1.49	1.37	74	14.1 / 6.4	77

rials: the BET specific surface area, S_{BET}, the total pore volume, V_t, the primary mesopore volume, V_p, the external surface area, S_{ext}, the diameters of pore entrances and internal parts estimated from desorption and adsorption branches, respectively. Analyzing the parameters presented in Table 1 one can find that prolongation of aging time increases the total and mesopore volumes and the pore diameters, however, it does not change the value of specific surface area, and decreases the share of silica skeleton in a total mass. The small-angle XRD patterns also shown in Fig. 1 reveal a structural transformation of PE9400-48h material during prolonged aging process in comparison to PE9400-24h sorbent. In the case of both silicas well-resolved peaks confirm the regular arrangement of their pores. However, the sample PE9400-24h shows the existence of only 3 peaks, while for the material PE9400-48h 4 reflections are found. It is difficult to determine a space group without any uncertainty, but undoubtedly the $F4_132$ fulfils the indices rules. For these samples and also for the rest ones discussed in this paper the cell parameter a was calculated for the F cubic structure.

The next group of PE materials was synthesized at 70°C for different polymer—TEOS mass ratios: 1:3.5, 1:3 and 1:2.5 (PE10500-1, PE10500-2, and PE10500-3). The nitrogen adsorption/desorption isotherms corresponding to the obtained samples are compared in Fig. 2. The successive increase of adsorption values in the range of higher relative pressures is observed with the growth of silica content in a reacting mixture; however, a shape of all isotherms is identical. Analysing the values of structure parameters presented in Table 1 one can find the increase of pore volumes, and insignificant growth of pore diameters. The XRD patterns presented in Fig. 2 for all obtained samples indicate the successive changes of pore arrangement with the increase of content of silica source. In the case of the sample PE10500-1 two reflections are observed; they become more distinct for the material PE9400-2 indicating an increase of pore system organization. The XRD curves indicate that the samples PE10500-1, PE10500-2, and PE10500-3 show worse ordering of structure in comparison to previously described samples (see Fig. 1).

In order to analyse the effect of pore structure on adsorption kinetics, especially in relation to the sizes of pore openings which may delay a transport of larger molecules into the internal cages, the kinetic measurements were undertaken for methylene blue adsorption. In Fig. 3 the nitrogen adsorption/desorption isotherms and pore size distributions calculated from adsorption and desorption branches of isotherms, are drawn for three samples of differentiated structure characteristics: PE9400-70 (the sample synthesized in standard conditions and aged at 70°C), PE9400-120 (the sample synthesized in standard conditions and aged at 120°C), and PE9400-90/48 (the simplified code PE9400-48h is used in Table 1). Strong shifts of desorption branches of the isotherms corresponding, respectively, to the sorbents PE9400-70, PE9400-90/48, and PE9400-120 indicate

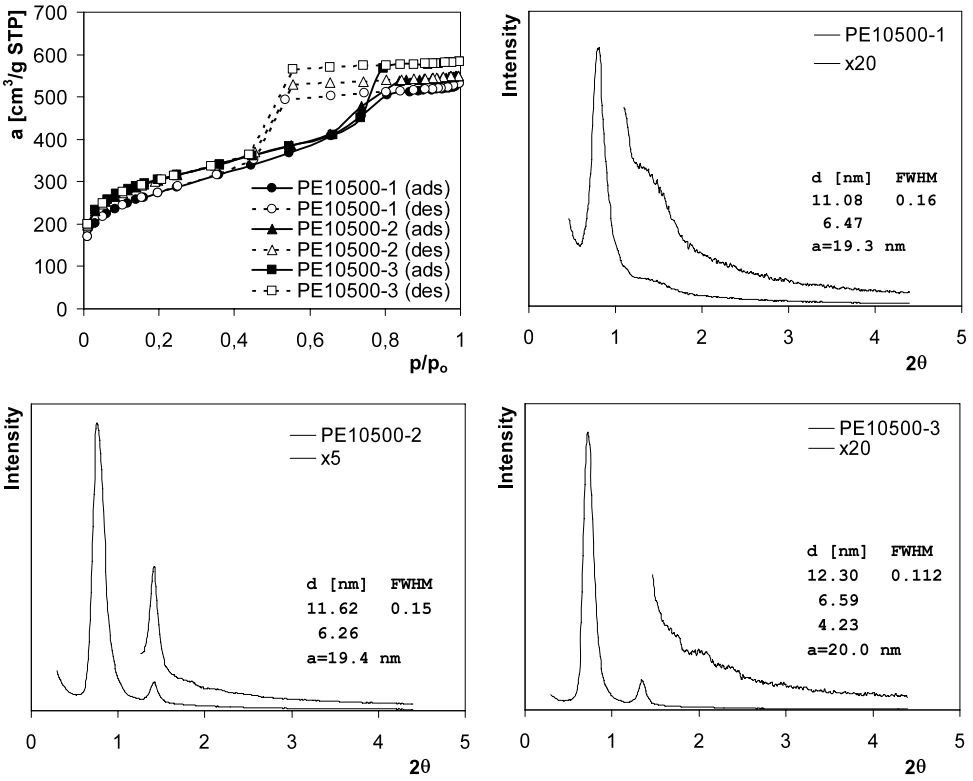

Fig. 2 Nitrogen adsorption/desorption isotherms and small-angle XRD patterns for the mesoporous silicas synthesized on the Pluronic PE10500 template at different mass ratios of polymer to TEOS

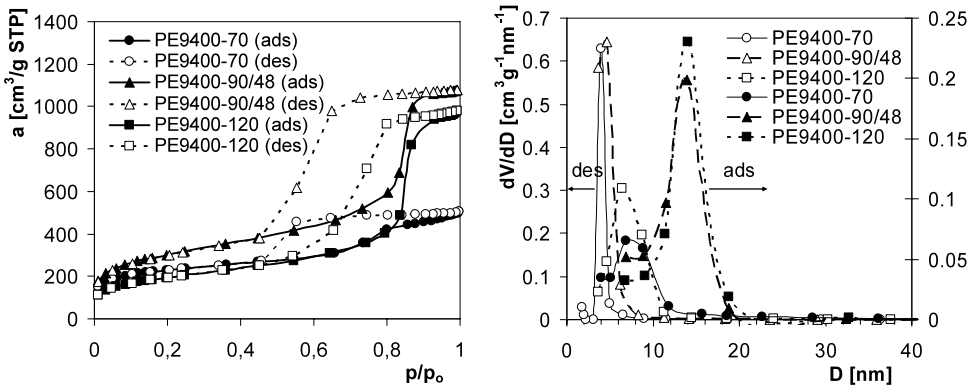

Fig. 3 Nitrogen adsorption/desorption isotherms and pore size distributions for the mesoporous silicas used in kinetic measurements

widening of pore entrances with aging temperature or time. This is well visible on the PSDs which are successively shifted on the diameter axis. The values of parameters characterizing these materials are given in Table 1; they reveal strong changes of pore volumes and diameters with synthesis conditions.

The obtained kinetic curves are presented in Fig. 4 as the ratio of temporary concentration C to the initial one, C_0, *versus* experiment time, t (total 14 hrs). In the first figure one may see a sudden drop of concentration at the start of experiment and then an exponential decrease of concentration. In the *log*-plots of concentration profiles the exponential character of the process and differences in the adsorption rates and are better visible. Such behaviour is characteristic for the pseudo-first order kinetics (Ho and McKay 1999a). Because of the complicated structure of our materials we fitted multi-exp equation corresponding to a series of parallel first order processes and the same parameters were used for calculation of adsorption curve, $a(t)$ (Marczewski 2007, 2008; Brandt et al. 2007):

$$C/C_0 = \sum_{i=1}^{s} A_i \exp(-k_i t) + A_0 \quad \text{where} \quad \sum_{i=1}^{s} A_i = 1 - A_0 \tag{1}$$

$$a = \frac{C_0 V}{m}\left[(1 - A_0) - \sum_{i=1}^{s} A_i \exp(-k_i t)\right] \tag{2}$$

where m is the adsorbent mass and V is the solution volume (the other parameters are explained below).

Table 2 Fitted parameters for multi-exponential kinetic curves, (1)

Sample	Fast stage			Slow stage			Equil.	Fast/slow	SD_{rel}[a]
	A_1	k_1	A_2	k_2	A_3	k_3	A_0	$A_1/(A_2+A_3)$	
PE9400-70	0.409	0.453	0.563	0.0053	0	0	0.0280	0.73	0,00206
PE9400-90/48	0.277	0.379	0.709	0.0069	0	0	0.0137	0.39	0,00201
PE9400-120	0.728	0.462	0.123	0.0070	0.134	0.0026	0.0150	2.83	0,00054

[a] $SD_{rel} = \frac{1}{C_o}\sqrt{\frac{1}{n-p}\sum_{i=1}^{n}(C_i - C_{fit}(t))^2}$ where n-number of kinetic points, $p = 2s + 1$-number of fitted parameters

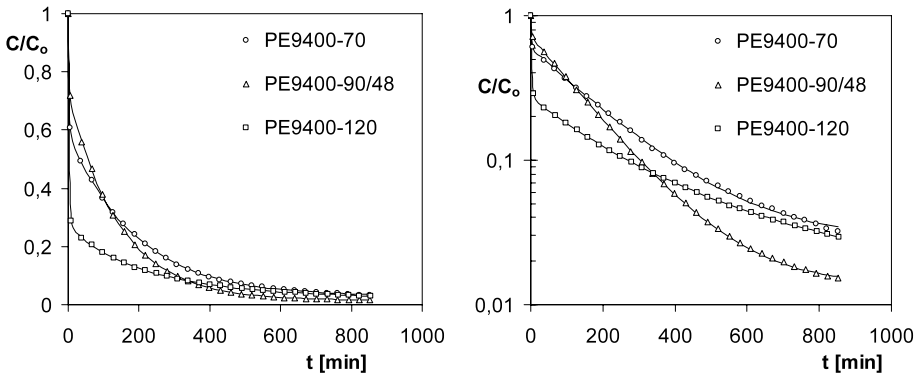

Fig. 4 Relative equilibrium concentration–time profiles of methylene blue adsorption from aqueous phase on the mesoporous silicas (*curves*—fitted lines, see Table 2)

We also tried to fit other kinetic equations (Ho and McKay 1999b; Moon and Lee 1983); however, (1) was the only one which could fit almost perfectly the entire kinetic experiment. It has to be noted that the fitting was unconstrained one and always reached the same set of parameters.

The results of fitting are shown in Table 2. The parameters A denote the total relative concentration change whereas the k describes the adsorption rate. The value A_0 allows to calculate (extrapolate) equilibrium concentration C_{eq} and adsorption a_{eq}. A_0 is the biggest (the smallest adsorption) for the sample PE9400-70 which has relatively small pore volume and surface area; A_0 is the smallest (the largest adsorption) for the material PE9400-90/48 which has the highest pore volume and surface area. The other parameters are divided into two groups: *fast* and *slow* stage parameters. The fast stage parameters (A_1 and k_1) describe the initial sudden drop of concentration (first 5–10 minutes). Similar values of the parameter k_1 show similar character of this process for all samples, however the total amount adsorbed in this fast process (A_1) is totally different. This difference may be associated with the difference in amount of pores which may be directly accessed from the adsorbent grain surface and it is clearly the largest for PE9400-120 which has the largest pores and large pore volume.

The slow stage parameters describe slow decrease of concentration which requires transport of adsorbate molecules through the narrower pores, longer channels or pore interconnectivities. The kinetic parameters k_2 are also similar for all investigated materials, though, for PE9400-70 is the smallest evidencing the narrowest pore openings of this sample. For PE9400-120 another slow process appears characterized by an even slower kinetics (A_3, k_3) which may seem strange because of its largest pores, however, it has also high pore volume which suggests that some pores might be available only through interconnectivities (the pore analysis does not reflect the pore length). The *fast/slow*-adsorption capacities' ratio (Table 2) is low for the PE9400-70 having small pores and small pore volume, the smallest for the sample PE9400-90/48 having the largest pore volume and by far the largest for PE9400-120. It is clear that during the pore development process they are widened as well as new pores are exposed through creation of new openings and interconnectivities and widening of the existing ones. The smallest *fast/slow* ratio for PE9400-90/48 where new pores appear is clear evidence of this supposition. Further thermal treatment dissolves some wall material what results in the destruction of some pores but mainly in widening access to all other pores and making access to them much easier.

In Fig. 5 the adsorption kinetics is shown as the time dependence of adsorption. The total adsorption values are not much different, though they do correspond to different equilibrium concentrations. However, the differences in the fast and slow stage adsorption processes are very well visible. Lines are drawn according to (2) and fitted parameters (Table 2).

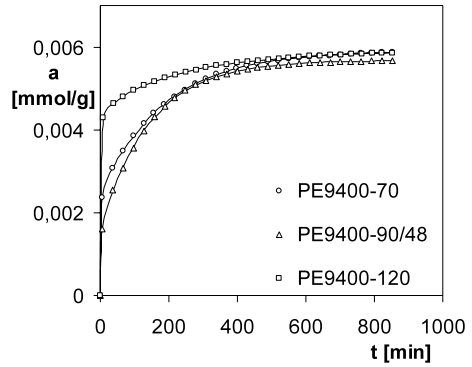

Fig. 5 Methylene blue adsorption from the aqueous phase on the mesoporous silicas vs. time

4 Conclusion

Some of the synthesized mesoporous silica materials show high structure ordering of *F* cubic type. Prolongation of aging process time increases the pore volume and diameter. Adsorption kinetics of methylene blue may be approximated by a series of first-order kinetic equations. The similarity of adsorption rate parameters indicates similar character of kinetic processes with weak dependence on the differences in pore structure characteristics of adsorbents. The differences in the kinetic curves may be associated with the varying amount and connectivity of pores.

Acknowledgement We thank BASF Poland for free samples of Pluronic polymers.

References

Brandt, A., Bülow, M., Derylo-Marczewska, A., Goworek, J., Schmeißer, J., Schöps, W., Unger, B.: Novel zeolite composites and consequences for rapid sorption processes. Adsorption **13**(3–4), 267–279 (2007)

Coleman, N.R.B., Morris, M.A., Spalding, T.R., Holmes, J.D.: The formation of dimensionally ordered silicon nanowires within mesoporous silica. J. Am. Chem. Soc. **123**(1), 187–188 (2001)

Derylo-Marczewska, A., Marczewski, A.W., Skrzypek, I., Pikus, S., Kozak, M.: Effect of aging temperature on structure characteristics of ordered mesoporous silicas. Appl. Surf. Sci. **252**(3), 625–632 (2005)

Derylo-Marczewska, A., Marczewski, A.W., Skrzypek, I., Pikus, S.: Effect of block copolymer type on formation of mesoporous silica structure. Pol. J. Chem. **82**, 205–212 (2008)

Gregg, S.J., Sing, K.S.W.: Adsorption, Surface Area and Porosity. Academic Press, London (1982)

Han, Y., Xiao, F.-S., Wu, S., Sun, Y., Meng, X., Li, D., Lin, S., Deng, F., Ai, X.: A novel method for incorporation of heteroatoms into the framework of ordered mesoporous silica materials synthesized in strong acidic media. J. Phys. Chem. B **105**(33), 7963–7966 (2001)

Hartmann, M., Vinu, A.: Mechanical stability and porosity analysis of large-pore SBA-15 mesoporous molecular sieves by mercury porosimetry and organics adsorption. Langmuir **18**(21), 8010–8016 (2002)

Ho, Y.S., McKay, G.: The sorption of lead(II) ions on peat. Water Res. **33**(2), 578–584 (1999a)

Ho, Y.S., McKay, G.: Pseudo-second order model for sorption processes. Process Biochem. **34**, 451–465 (1999b)

Huang, T.C., Toraya, H., Blanton, T.N., Wu, Y.: X-ray powder diffraction analysis of silver behenate, a possible low-angle diffraction standard. J. Appl. Cryst. **26**(2), 180–184 (1993)

Janssen, A.H., Van Der Voort, P., Koster, A.J., de Jong, K.P.: A 3D-TEM study of the shape of mesopores in SBA-15 and modified SBA-15 materials. Chem. Commun. **15**, 1632–1633 (2002)

Jaroniec, M., Kruk, M., Olivier, J.P.: Standard nitrogen adsorption data for characterization of nanoporous silicas. Langmuir **15**(16), 5410–5413 (1999)

Krämer, E., Förster, S., Göltner, Ch., Antonietti, M.: Synthesis of nanoporous silica with new pore morphologies by templating the assemblies of ionic block copolymers. Langmuir **14**(8), 2027–2031 (1998)

Kruk, M., Antochshuk, V., Matos, J.R., Mercuri, L.P., Jaroniec, M.: Determination and tailoring the pore entrance size in ordered silicas with cage-like mesoporous structures. J. Am. Chem. Soc. **124**(5), 768–769 (2002)

Lettow, J.S., Han, Y.J., Schmidt-Winkel, P., Yang, P., Zhao, D., Stucky, G., Ying, J.Y.: Hexagonal to mesocellular foam phase transition in polymer-templated mesoporous silicas. Langmuir **16**(22), 8291–8295 (2000)

Marczewski, A.W.: Kinetics and equilibrium of adsorption of organic solutes on mesoporous carbons. Appl. Surf. Sci. **253**(13), 5818–5826 (2007)

Marczewski, A.W.: Kinetics and equilibrium of adsorption of dissociating solutes from aqueous solutions on mesoporous carbons. Pol. J. Chem. **82**, 271–281 (2008)

Matos, J.R., Mercuri, L.P., Kruk, M., Jaroniec, M.: Synthesis of large-pore silica with cage-like structure using sodium silicate and triblock copolymer template. Langmuir **18**(3), 884–890 (2002)

Melosh, N.A., Davidson, P., Feng, P., Pine, D.J., Chmelka, B.F.: Macroscopic shear alignment of bulk transparent mesostructured silica. J. Am. Chem. Soc. **123**(6), 1240–1241 (2001)

Moon, H., Lee, W.K.: Intraparticle diffusion in liquid-phase adsorption of phenols with activated carbon in finite batch adsorber. J. Colloid Interface Sci. **96**(1), 162–171 (1983)

Newalkar, B.L., Komarneni, S.: Simplified synthesis of micropore-free mesoporous silica. SBA-15, under microwave-hydrothermal conditions, Chem. Commun. **16**, 1774–1775 (2002)

Sakamoto, Y., Kaneda, M., Terasaki, O., Zhao, D.Y., Kim, J.M., Stucky, G.D., Shin, H.J., Ryoo, R.: Direct imaging of the pores and cages of three-dimensional mesoporous materials. Nature **408**(6811), 449–453 (2000)

Schmidt-Winkel, P., Lukens, W.W. Jr., Zhao, D., Yang, P., Chmelka, B.F., Stucky, G.D.: Mesocellular siliceous foams with uniformly sized cells and windows. J. Am. Chem. Soc. **121**(1), 254–255 (1999a)

Schmidt-Winkel, P., Yang, P., Margolese, D.I., Chmelka, B.F., Stucky, G.D.: Fluoride-induced hierarchical ordering of mesoporous silica in aqueous acid-syntheses. Adv. Mater. **11**(4), 303–307 (1999b)

Schmidt-Winkel, P., Glinka, Ch.J., Stucky, G.D.: Microemulsion templates for mesoporous silica. Langmuir **16**(2), 356–361 (2000)

Yu, C., Yu, Y., Zhao, D.: Highly ordered large caged cubic mesoporous silica structures templated by triblock PEO–PBO–PEO copolymer. Chem. Commun. **7**, 575–576 (2000)

Zhao, D., Huo, Q., Feng, J., Chmelka, B.F., Stucky, G.D.: Nonionic triblock and star diblock copolymer and oligomeric surfactant syntheses of highly ordered. Hydrothermally stable, mesoporous silica structures, J. Am. Chem. Soc. **120**(24), 6024–6036 (1998)